Brain Stimulation 18 (2025) 1966–1977

Contents lists available at ScienceDirect

Brain Stimulation

journal homepage: www.journals.elsevier.com/brain-stimulation

Anodal M1 tDCS shapes frequency-specific functional connectivity and network topology in Parkinson's disease

Clara Simonetta [a,1], Matteo Conti [a,*,1], Jacopo Bissacco [a], Valerio Ferrari [a], Chiara Salimei [b], Federico Carparelli [a], Silvio Bagetta [a], Davide Mascioli [a], Veronica Buttarazzi [a], Maria Mancini [a], Francesca Di Giuliano [c], Nicola Biagio Mercuri [a], Mariangela Pierantozzi [a], Alessandro Stefani [a], Tommaso Schirinzi [a]

[a] Neurology Unit, Department of Systems Medicine, University of Rome "Tor Vergata", Rome, Italy
[b] Department of Clinical Sciences and Translational Medicine, University of Rome "Tor Vergata", Rome, Italy
[c] Neuroradiology Unit, Department of Biomedicine and Prevention, University of Rome "Tor Vergata", Rome, Italy

ARTICLE INFO

Keywords:
Parkinson's disease
Transcranial direct current stimulation
High-density EEG
Functional connectivity
Graph theory
Intermediate-stage Parkinson's disease

ABSTRACT

Background: Transcranial direct current stimulation (tDCS) is a promising non-invasive intervention for Parkinson's disease (PD), but its mechanisms of action remain unclear. Understanding its network-level effects may support its use as an adjunctive therapeutic option, particularly in intermediate-stage PD when symptoms begin to escape pharmacological control.

Objective: To evaluate the clinical efficacy and functional connectivity (FC) changes of anodal tDCS over the primary motor cortex (M1) in patients with intermediate-stage PD.

Methods: Twenty-five patients underwent a randomized, double-blind, sham-controlled, crossover protocol, receiving anodal and sham M1-tDCS. Clinical assessments were measured before and after each intervention, alongside high-density EEG (HD-EEG) recordings in the OFF-medication state. Band-specific FC was analyzed using network-based statistics (NBS), and network topology was examined through graph-theoretical measures. Thirty age-matched healthy controls were included for baseline comparisons.

Results: anodal tDCS significantly reduced motor symptoms in the OFF-state, especially bradykinesia, tremor, and gait. It also improved non-motor symptoms and cognitive performance. HD-EEG FC analyses revealed increased α-band FC and decreased pathological β-band hyperconnectivity, both correlating with clinical improvements. Notably, graph analyses showed reduced scale-free organization in both α- and β-band networks post-tDCS, likely reflecting the widespread and non-selective stimulation of multiple nodes. Sham stimulation induced no significant changes.

Conclusions: Therapeutic effects of anodal M1-tDCS appear to be mediated by frequency-specific modulation of cortical networks, enhancing α-band synchronization and reducing β-band hypersynchrony, alongside a topological reconfiguration of brain architecture. These network-level effects strengthen the rationale for using tDCS in PD, particularly as a potential therapeutic option in the intermediate stage.

1. Introduction

Parkinson's disease (PD) is a common neurodegenerative disorder, characterized by the degeneration of dopaminergic neurons in the substantia nigra and intraneuronal accumulation of α-synuclein [1]. However, PD is rather a multisystem condition involving widespread dysfunction across subcortical and cortical networks [2], leading to a heterogeneous clinical presentation with both motor and non-motor symptoms. In the early stages, dopaminergic therapies provide satisfactory symptom control. In intermediate and advanced stages, the emergence of motor fluctuations and the worsening of symptoms poorly responsive to therapy lead to a deterioration in quality of life. Device-assisted therapies (DATs) offer substantial benefit in advanced patients [3]. However, they cannot be offered to all patients at the first

* Corresponding author. Department of Systems Medicine, Unit of Neurology University of Rome Tor Vergata, Via Montpellier, 00133, Rome, Italy.
E-mail address: matteoconti92@gmail.com (M. Conti).
[1] The authors contributed equally as first.

https://doi.org/10.1016/j.brs.2025.10.016
Received 30 July 2025; Received in revised form 2 October 2025; Accepted 21 October 2025
Available online 26 October 2025

appearance of disabling symptoms, as eligibility criteria restrict access. Moreover, these interventions may not adequately address certain symptoms, such as gait disturbances and cognitive impairment. This highlights the need for alternative therapeutic strategies that can bridge patients along the path to DAT eligibility, substitute DATs when contraindicated, or complement oral medications when symptom burden increases and is no longer adequately controlled by conventional treatment [4].

In this context, non-invasive neuromodulation may represent a viable strategy due to its low cost, ease of use, and favorable safety profile. Within this context, both transcranial direct current stimulation (tDCS) and transcranial alternating current stimulation (tACS) have been explored. According to available evidence, tDCS presents higher feasibility for repeated daily applications and greater capacity to induce sustained plasticity-related changes in cortical excitability [5], whereas tACS primarily targets oscillatory entrainment [6]. Several works reported an improvement in motor function [7–11], gait and balance [10,12,13], cognitive performance [14–16], other non-motor symptoms [17], and impulse control disorders [18] of PD patients receiving various tDCS protocols. However, other studies have failed to replicate these clinical benefits [19–23], leading to mixed meta-analytic findings [24–27]. This variability likely reflects heterogeneity in stimulation targets, protocols, outcome measures, and patient stages, as well as the inherent variability in individual responsiveness to non-invasive brain stimulation. Indeed, the mechanisms of action and the biological bases of tDCS are still poorly understood. Early studies demonstrated that low-intensity electrical stimulation is capable of modulating cortical excitability without reaching the action potential threshold [28,29], inducing long-term synaptic plasticity [30]. Yet, how such excitability changes translate into improvement of multidimensional symptoms remains unclear.

The analysis of functional connectivity (FC) based on high-density electroencephalography (HD-EEG) enables the sensitive detection of cortical integration changes with high temporal resolution and adequate spatial accuracy. This technique helped define a neurophysiological profile of the disease, with band- and network-specific abnormalities associated with key motor and non-motor symptoms [31,32,69]. The EEG-based FC might thus represent a valuable tool to investigate cortical network dynamics in response to neuromodulation, opening a window on the biological effects of the tDCS.

Clinical applications of EEG-based FC might be further implemented by a graph theoretical approach, where brain regions are represented as nodes and their interactions as edges [33–35]. This approach can capture key topological properties of brain networks, which, like many biological systems, often exhibit a scale-free architecture, a configuration considered fundamental to the brain's resilience and efficiency [36]. In PD, the network organization is disrupted [37,38], compromising the brain's capacity for efficient information transfer and integration across regions.

In this study, we aimed to evaluate the clinical and neurophysiological effects of an anodal tDCS protocol targeting the primary motor cortex (M1) in PD patients at an intermediate stage of the disease. Notably, this phase was chosen as it represents a potentially optimal window for non-invasive neuromodulation, when dopaminergic treatment alone begins to lose efficacy while patients are not yet eligible for DATs. We thus conducted a single-center, randomized, sham-controlled, cross-over study, using both clinical outcomes and HD-EEG recordings, the latter to detect changes in cortical extrinsic FC and network organization induced by neuromodulation. A group of age-matched healthy controls (HCs) was also included to provide baseline references for FC and graph-based network metrics.

2. Materials and methods

2.1. Study subjects

25 right-handed patients with idiopathic PD were enrolled (2022–2024) from the Movement Disorders Clinic of "Tor Vergata" University Hospital in Rome, Italy. Inclusion criteria were: diagnosis of idiopathic PD per 2015 Movement Disorders Society diagnostic criteria [39] and absence of PD dementia [40]. Patients were in an intermediate stage, with $\geq$5 years of disease duration and early motor fluctuations (before the so-called advanced phase as defined by the 5-2-1 criteria [41,42]). Exclusion criteria included tDCS contraindications (intracranial devices, metallic implants, pacemakers) [43]; epilepsy or other EEG-interfering neurological disorders, and acute or unstable medical conditions. All patients maintained a stable pharmacological regimen for $\geq$1 month before and throughout the study. 30 age- and sex-matched healthy controls (HC) were enrolled for comparison. The study followed the Declaration of Helsinki and received ethical approval (protocol no. 190/18); all participants gave written informed consent.

2.2. Experimental design

We designed a randomized, double-blind, sham-controlled, cross-over study (Fig. 1). Each PD patient received both active and sham stimulation in a randomized order. Clinical and neurophysiological evaluations were performed before the first stimulation session (T0) and after the final session (T1) of each cycle. Clinical outcomes included motor and non-motor assessments. Neurophysiological outcomes were assessed through 64-channel high-density EEG (HD-EEG) recordings acquired in the OFF state, to prevent confounding effects of dopaminergic medication. EEG data were used to compute source-level functional connectivity and graph-theoretical network measures, as described below.

2.3. tDCS stimulation protocol

All participants received active and sham anodal tDCS in 2-week cycles of 10 daily-sessions (20 min/session), with a minimum 3-month washout to avoid carryover effects. Stimulation was delivered via a constant-current device (BrainSTIM, EMS) using 25 cm^2 saline-soaked sponge electrodes with anode over left M1 (C3) and cathode over right supraorbital ridge (Fp2) [44]. A 2.0 mA current was applied during active sessions; in sham, the current was stopped after 40 s. Both conditions included 5-s ramp-up/down phases. Stimulation occurred in the ON-medication state, consistent with most previous trials and supported by evidence of a synergistic interaction between dopaminergic therapy and tDCS in promoting long-lasting effects [45]. Both subjects and investigators were blinded, and adverse events were monitored throughout.

2.4. Clinical assessment

At baseline, all patients were assessed for demographic and clinical data, Hoehn&Yahr (HY) stage, and levodopa equivalent daily dose (LEDD) [46]. Motor symptoms were evaluated using MDS-UPDRS partIII scores, in both OFF (after overnight therapy withdrawal) and ON-medication states. Subscores were derived for rigidity (item 3.3), bradykinesia (items 3.4–3.8), tremor (items 3.15–3.18), and gait (items 3.9–3.12) [47]. Non-motor symptoms were evaluated using the Non-Motor Symptoms Scale (NMSS) [48] and the PD-Cognitive Rating Scale (PD-CRS) [49].

2.5. HD-EEG data acquisition

All participants underwent 64-channel HD-EEG. Patients were evaluated pre- and post-stimulation in OFF-medication state. HD-EEG

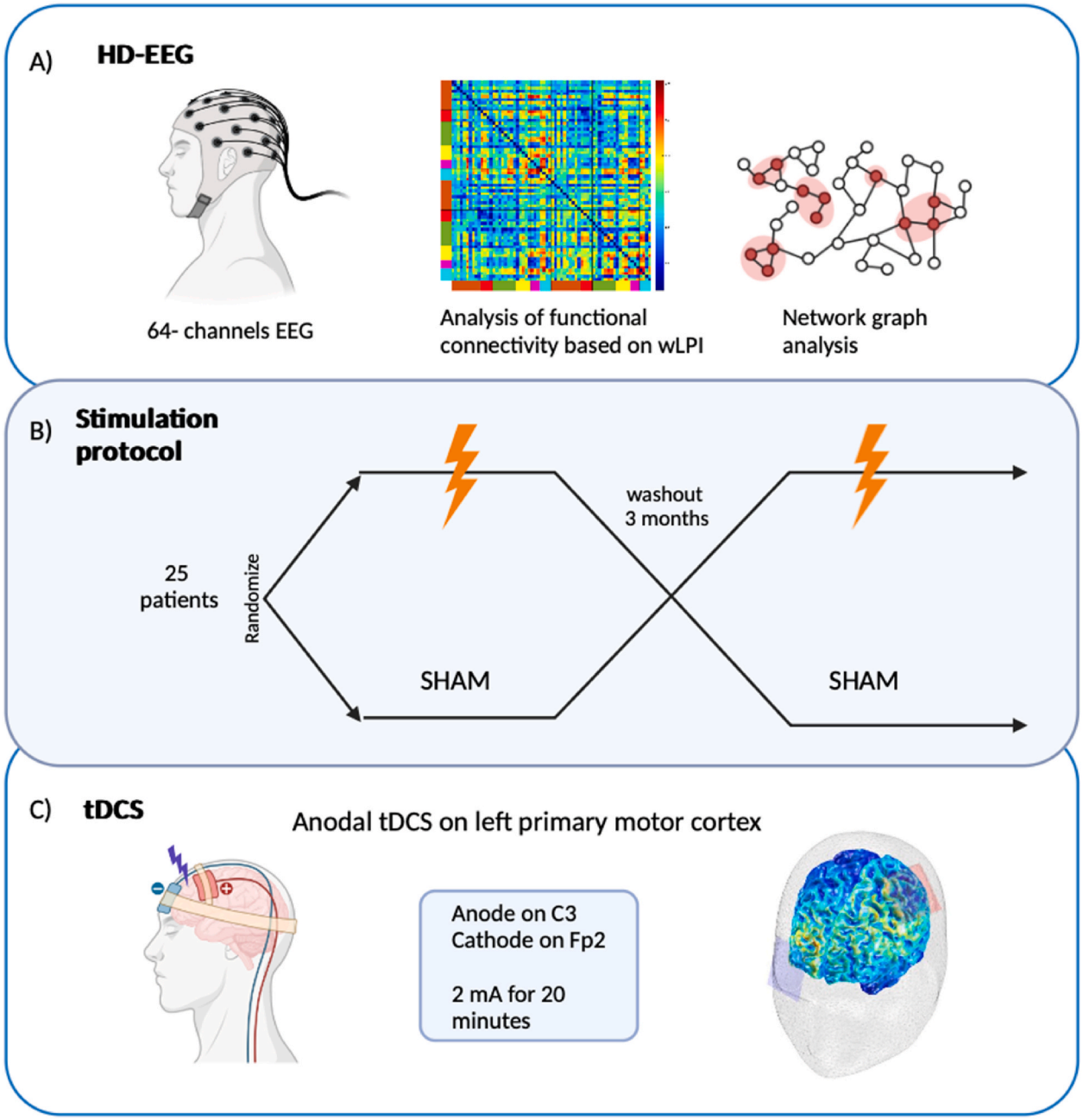

Fig. 1. A) HD-EEG signal acquisition from 64 channels, followed by functional connectivity analysis using weighted Lagged Phase Index (wLPI) and network graph analysis; B) Schematic representation of the randomized, sham-controlled, crossover stimulation protocol with anodal tDCS; C) tDCS montage with corresponding current density map. Figure created with BioRender.com.

was recorded for 10 min at 1024 Hz, bandpass-filtered (0.5–50 Hz), using a BePlus ProStandard system (EBNeuro, Florence, Italy), following the 10–10 system with impedance <5 kΩ. Reactivity to eye opening and activation tests were performed to exclude epileptiform elements. Recordings were segmented into 30 s epochs each [50]. After discarding the first epoch, six consecutive epochs (180s total) were retained. Independent component analysis (ICA) was used to remove the residual EEG artifacts [51]. EEG source localization was performed based on personal MRI. FC was calculated in source space using weighted phase lag index (wPLI) [52] in θ (4–8 Hz), α (8–13 Hz), β (13–30 Hz), and low-γ (30–50 Hz) bands. Details on the estimation of source activity and FC analysis are provided in the Supplementary Materials.

2.6. Standard statistical analysis

Descriptive statistics were calculated. Clinical effects were assessed by comparing T0 and T1 scores within each arm (anodal vs. sham) using paired t-tests or Wilcoxon tests, based on data distribution.

2.7. NBS analysis and Machine Learning optimization

FC changes in θ, α, β, and low-γ bands were evaluated using Network-Based Statistic (NBS), a cluster-based method with higher power than univariate tests [53]. We first compared PD patients and HC at T0 to identify baseline FC differences; then, we assessed pre-post tDCS effects within the PD group. Mean network connectivity (mNC) was computed as the average FC within the identified differential networks. A

two-sample *t*-test was used to evaluate differences in mNC between groups. Moreover, Spearman's rank correlation was used to relate mNC to clinical measures both at baseline and for change scores (ΔmNC and Δclinical scores from T1–T0), quantifying stimulation-related effects. All correlations were corrected for multiple comparisons using the false discovery rate (FDR) method. Further details on NBS analysis and Machine Learning (ML) optimization are provided in the Supplementary Materials.

2.8. Graph theory analysis

We examined the intrinsic organization of whole-brain FC in HC and PD patients using graph theoretical approaches. We computed three global graph metrics to characterize whole-brain network organization: transitivity (a measure of functional segregation), global efficiency (an index of functional integration), and assortativity (a marker of network resilience). Moreover, the scale-freeness of the networks was explicitly assessed. Full methodological details are reported in the Supplementary Materials.

Statistical analyses and graphs were performed using SPSS, R (ggplot2), MATLAB 2024a, and NBS toolbox [64]; ML analyses were conducted in MATLAB (Statistics and Machine Learning Toolbox). The significance threshold was set at $p \leq 0.05$.

A priori power analysis was conducted for our study, using G*Power 3.1 [54]. Power calculation was computed for the linear generalized model, on which NBS is based. For the between-group comparison (PD patients, n = 25 vs. HC, n = 30), an independent-samples *t*-test was used. Assuming a large effect size (Cohen's d = 0.8), a two-tailed α of 0.05, the analysis indicated that 52 subjects would be required to achieve 80 % power. For the within-patient comparison (pre-vs. post-tDCS, n = 25), a paired-samples *t*-test was used. Under the same assumptions, 15 subjects were required to achieve 80 % power. Thus, the sample size can be considered adequate to detect large effects with at least 80 % power.

3. Results

3.1. Demographic analysis

Table 1 summarizes the main clinical and demographic parameters of HC and PD groups.

3.2. NBS analysis of band-specific FC between PD and HC

Through NBS, we found networks at the α-band (t 2.0–3.9), where the FC was significantly lower in PD patients than in HC. SVM algorithm identified the optimal network differentiating PD patients from HC at t = 3.7 ($p < 0.001$) (accuracy 0.87 [IC95 % 0.83–0.89], AUC 0.95 [IC95 % 0.87–0.99], sensitivity 0.92 [IC95 % 0.74–1.00], specificity 0.87 [IC95 % 0.69–0.96]) (Fig. 2, Panels C). This network comprised 39 nodes and 47 links, balanced across hemispheres (left 51.1 %). ROIs with higher degrees were part of the orbitofrontal cortex (predominantly bilateral medial orbitofrontal and frontal pole), dorsolateral prefrontal cortex (mostly bilateral superior frontal and left caudal middle frontal), sensorimotor (mostly bilateral pre and postcentral areas), limbic (mainly bilateral anterior cingulate) and temporal (mostly left transverse temporal) lobes (Fig. 2, *Panels A-B*). The mNC of this network was significantly lower in PD than HC (t = −10.17, $p < 0.001$) (Fig. 2, Panel D).

Then, we analyzed correlations between the altered α FC network and clinical scores at baseline in the PD group. We found a significant negative correlation between the mNC of the α network and the gait/postural subscore of the MDS-UPDRS-III (r = −0.40, p = 0.04, BS-95 %CI [−0.66 0.10]) (Fig. 2, Panel E) and total NMSS score (r = −0.43, p = 0.03, BS-95 %CI [−0.72 -0.02]) (Fig. 2, Panel F), and a positive correlation between the mNC of the α network and PD-CRS score (r = 0.48, p = 0.02, BS-95 %CI [0.15 0.73]) (Fig. 2, Panel G).

Conversely, we found a set of networks at the β-band (t 2.0–4.1), characterized by hyperconnectivity in PD patients compared to HC. Using the ML algorithm, we selected the network t = 3.7 as the best classifier to distinguish PDs from HCs (accuracy 0.85 [IC95 % 0.82–0.87], AUC 0.90 [IC95 % 0.75–0.97], sensitivity 0.84 [IC95 % 0.64–0.96], specificity 0.90 [IC95 % 0.73–0.97]) (Fig. 2, Panels J). The network was composed of 33 nodes and 42 edges and was predominant in the left hemisphere (54.5 %). Brain regions with higher degrees were part of sensorimotor (mainly bilateral precentral and postcentral), limbic (predominantly bilateral anterior cingular and para-hippocampal cortex), parietal (Fig. 2, *Panels H-I*). Likewise, mNC was significantly higher in PD compared to HC (t = 6.3, $p < 0.001$) (Fig. 2, Panel K). Assessing the correlations between the β network and clinical scores in patients, we found a positive correlation between the mNC of the β network and MDS-UPDRS-III bradykinesia scores (r = 0.41, p = 0.04, BS-95 %CI [0.01 0.69]) (Fig. 2, Panel L). No significant group differences emerged in other frequency bands.

3.3. Graph-theoretical analysis of functional organization between PD and HC

We applied graph-theoretical analysis to the α-band FC-EEG in both groups to investigate the difference in intrinsic functional organization between PD patients and HC. Compared to HC, PD patients' whole-brain network showed reduced transitivity (PD 0.09 ± 0.04, HC 0.12 ± 0.03, p = 0.0046), and global efficiency (PD 0.07 ± 0.03, HC 0.18 ± 0.06, p = 0.0010), along with increased assortativity (PD -0.08 ± 0.10, HC -0.14 ± 0.10, p = 0.036). No significant difference was observed in scale-freeness (PD 0.65 ± 0.30, HC 0.71 ± 0.35, p = 0.56) (Fig. 3, Panel A).

A similar analysis was performed on the β band. Compared to HC, PD patients exhibited significantly higher transitivity (PD 0.06 ± 0.03, HC 0.04 ± 0.02, $p < 0.001$), greater global efficiency (PD 0.09 ± 0.05, HC 0.06 ± 0.03, p = 0.009). No differences were found in assortativity (PD -0.04 ± 0.07, HC -0.05 ± 0.08, p = 0.62) and scale-freeness (PD 0.70 ± 0.27, HC 0.71 ± 0.41, p = 0.92) (Fig. 3, Panel B).

3.4. Motor and non-motor effects of anodal tDCS in PD

Anodal stimulation significantly improved MDS-UPDRS III score in the OFF state (T0 26.26 ± 10.30 vs T1 24.76 ± 11.30, p = 0.009). Subdomain analysis revealed significant improvements in bradykinesia (T0 13.56 ± 6.35 vs T1 11.40 ± 6.38, p = 0.001), tremor (T0 3.78 ± 4.24 vs T1 2.28 ± 2.90, p = 0.011), and gait/posture (T0 2.28 ± 2.56 vs T1 1.92 ± 2.02, p = 0.038), with no changes in rigidity. No significant effects were observed in the ON state, although a mild trend toward reduction emerged. The stimulation improved NMSS (T0 32.76 ± 38.39 vs T1 24.16 ± 23.25, $p < 0.001$) and PD-CRS (T0 98.56 ± 17.62 vs T1 104.64 ± 14.20, p = 0.012). No significant changes were detected following sham stimulation. In patients who received real stimulation first, baseline scores at the start of the sham arm were compared with those at the start of the initial real arm and showed no statistically significant differences, indicating no carryover after the three-month washout.

Table 1
Demographic and Clinical Characteristics of Patients with Parkinson's Disease (PD) and Healthy Controls (HC). Disease duration and age are expressed in years. H&Y: Hoehn and Yahr staging of disease severity in PD. LEDD: Levodopa Equivalent Daily Dose (mg/day).

	PD (n = 25)	HC (n = 30)	pValue
Age (y)	59.04 ± 9.46	57.36 ± 10.12	n.s.
Sex (F/M)	7/18	12/13	n.s.
Disease duration (y)	5.77 ± 2.65	–	
H&Y stage	2.16 ± 0.31	–	
most affected side (L/R)	15/10	–	
LEDD (mg/day)	494.14 ± 266.11	–	

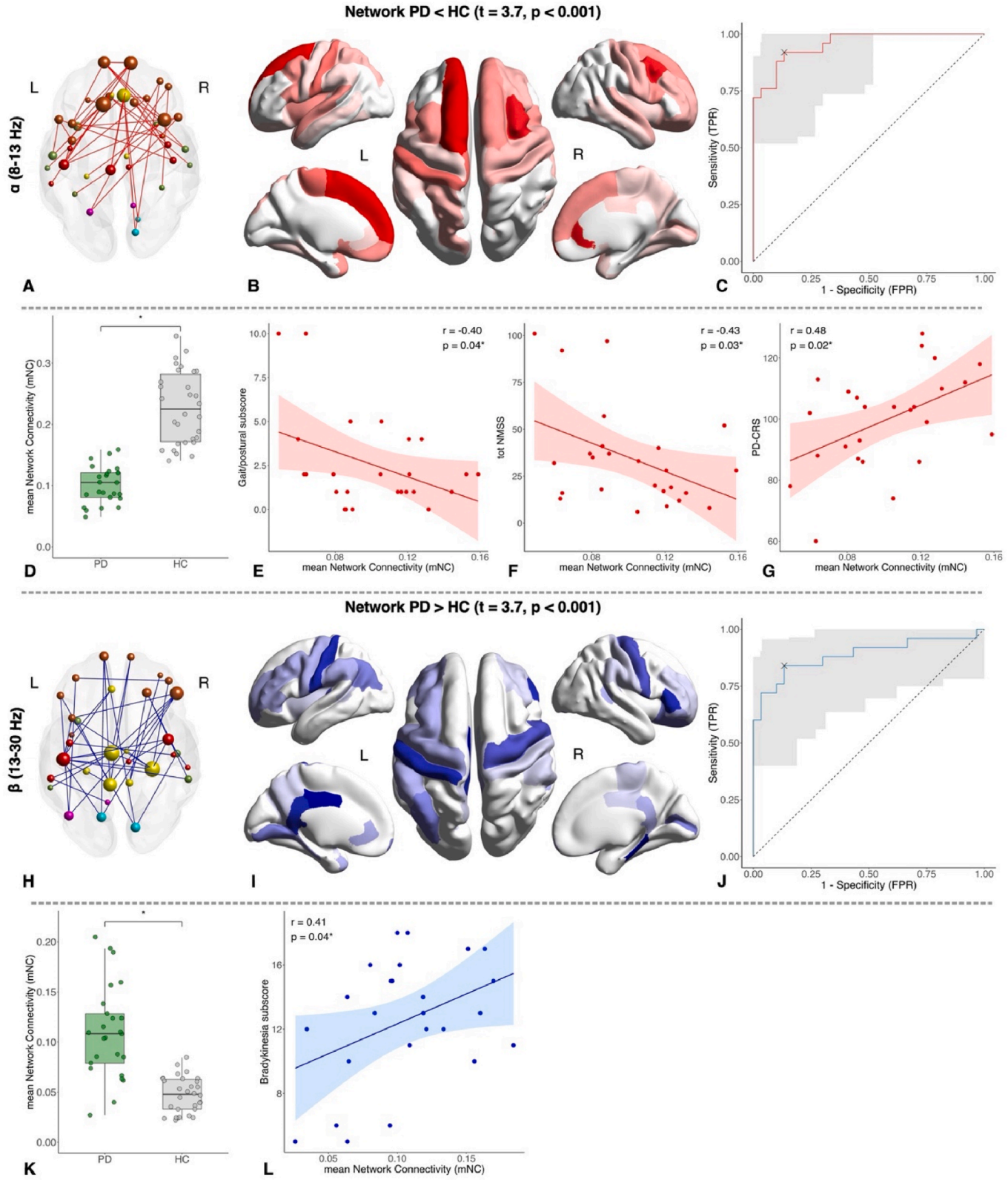

Fig. 2. Graph representation of the differential networks between PD patients and HC in α (**A**) and β (**H**) bands. The color of spheres represents different brain lobes: orange = fronto-insular, red = sensorimotor, yellow = limbic, green = temporal, magenta = parietal, light-blue = occipital; sphere diameters are directly proportional to region of interest (ROI) degrees. Map representation of ROI degrees on model brain surface of the differential networks in α (**B**) and β (**I**) bands. ROC curves indicating the predictive performance (PD vs HC) of the identified NBS network at α (**C**) and β (**J**) bands. Box plots represent the mNC values in PD and HC groups of the NBS networks in α (**D**) and β (**K**) bands. Spearman's correlation between mean network connectivity (mNC) of the α network and gait/postural subscore of MDS-UPDRS-III (**E**), tot NMSS (**F**), and PD-CRS (**G**). Spearman's correlation between the mean network connectivity (mNC) of the β network and the bradykinesia subscore of MDS-UPDRS-III (**L**).

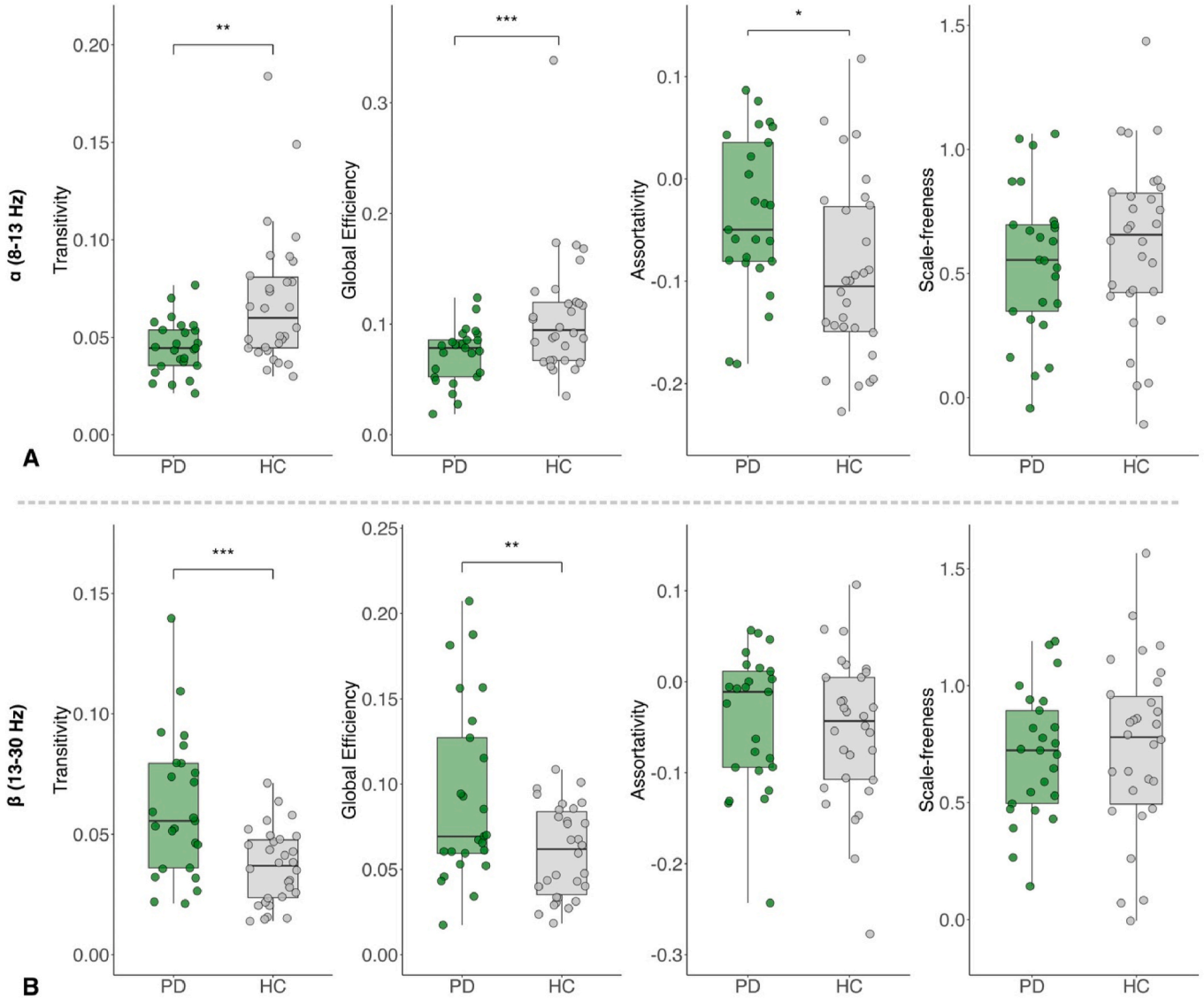

Fig. 3. Boxplots of global graph metrics (Transitivity, Global Efficiency, Assortativity, Scale-Freeness) comparing PD and HC in **(A)** α band network and **(B)** β band network. Statistical significance is indicated by asterisks: $p < 0.05$ (*), $p < 0.01$ (**), $p < 0.001$ (***).

Table 2
Clinical Outcomes of tDCS (Verum/Anodal vs Sham). T0: Baseline, T1: Post-treatment. MDS-UPDRS III: Movement Disorders Society—Unified Parkinson's Disease Rating Scale, Part III. NMSS: Non-Motor Symptoms Scale, PD-CRS: Parkinson's Disease Cognitive Rating Scale. Data are reported as Mean ± Standard Deviation of variables. Statistically significant p-values (<0.05) are highlighted in bold.

	PD patients (n = 25)					
	Verum			Sham		
	T0	T1	pValue	T0	T1	pValue
MDS-UPDRS-III OFF	26.26 ± 10.30	24.76 ± 11.30	**0.009**	27.08 ± 11.38	26.76 ± 10.96	0.879
Bradykinesia	13.56 ± 6.35	11.40 ± 6.38	**0.001**	11.56 ± 5.98	12.12 ± 5.98	0.200
Rigidity	4.22 ± 1.98	4.08 ± 2.47	0.167	4.32 ± 5.56	4.72 ± 2.26	0.094
Tremor	3.78 ± 4.24	2.28 ± 2.90	**0.011**	3.12 ± 3.92	3.32 ± 3.59	0.600
Gait/Postural	2.28 ± 2.56	1.92 ± 2.02	**0.038**	1.72 ± 2.41	1.92 ± 2.34	0.096
MDS-UPDRS-III ON	14.61 ± 7.88	14.52 ± 8.36	0.109	16.00 ± 10.35	16.36 ± 9.33	0.781
Bradykinesia	6.17 ± 4.19	6.32 ± 4.37	0.296	6.56 ± 5.41	6.92 ± 4.86	0.414
Rigidity	2.74 ± 1.82	2.24 ± 1.77	0.077	2.84 ± 2.08	2.52 ± 2.42	0.455
Tremor	1.70 ± 2.18	1.20 ± 1.94	0.151	1.52 ± 2.36	1.32 ± 2.08	0.716
Gait/Postural	1.32 ± 1.80	1.36 ± 1.63	0.869	1.88 ± 2.15	1.68 ± 2.06	0.197
NMSS	32.76 ± 38.39	24.16 ± 23.25	**<0.001**	33.04 ± 22.68	30.68 ± 24.71	0.072
PD-CRS	98.56 ± 17.62	104.64 ± 14.20	**0.012**	99.76 ± 15.90	101.84 ± 14.57	0.106

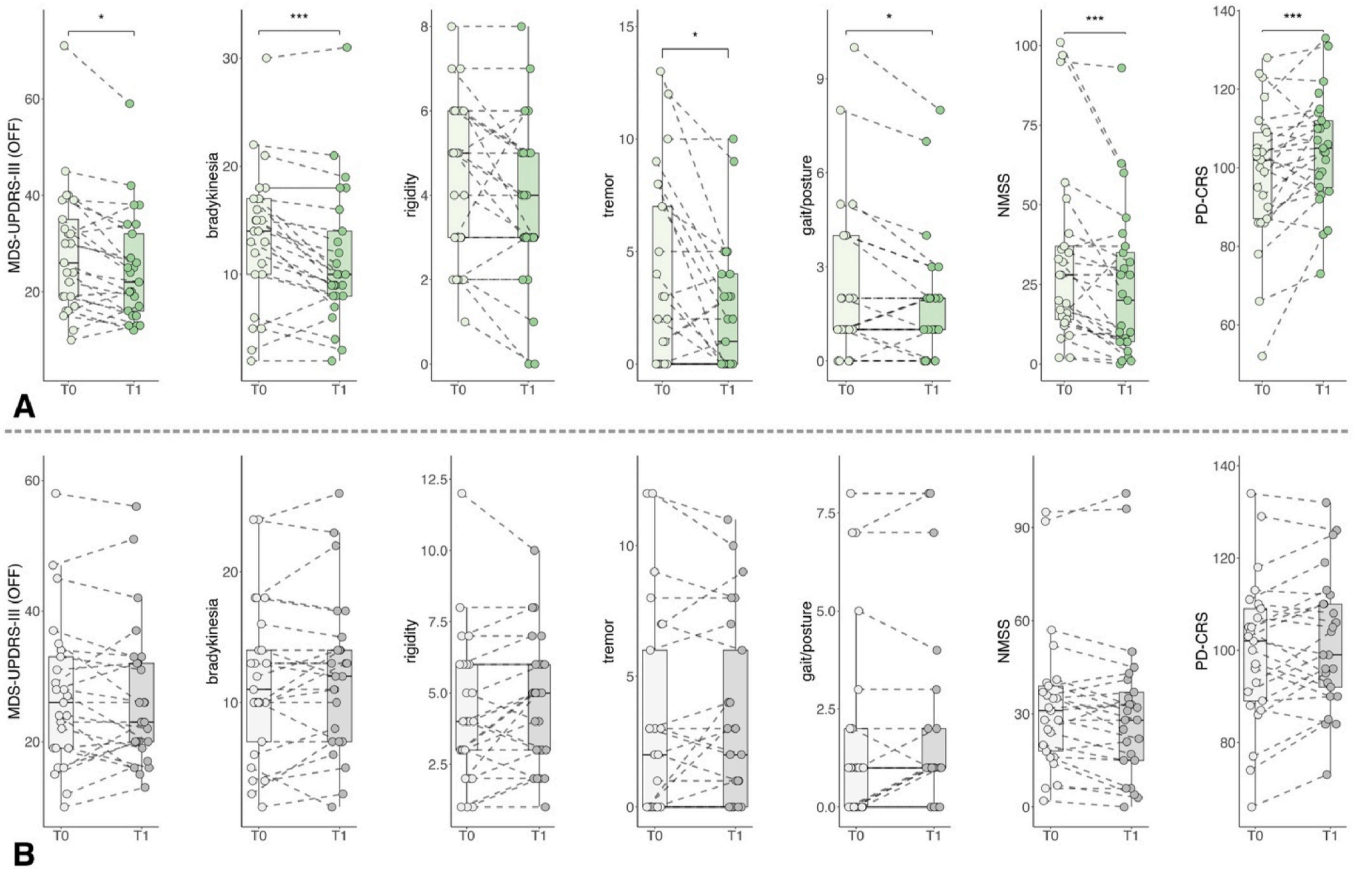

Fig. 4. Combined spaghetti and boxplots illustrating pre- (T0) and post-stimulation (T1) clinical scores. **(A)** Verum/Anodal tDCS; **(B)** Sham tDCS. MDS-UPDRS III: Movement Disorders Society—Unified Parkinson's Disease Rating Scale, Part III. NMSS: Non-Motor Symptoms Scale, PD-CRS: Parkinson's Disease Cognitive Rating Scale. Statistical significance is indicated by asterisks: $p < 0.05$ (*), $p < 0.01$ (**), $p < 0.001$ (***).

Complete clinical data are reported in Table 2 and Fig. 4.

3.5. NBS analysis of band-specific FC modulation induced by anodal tDCS in PD

In the verum tDCS–OFF condition, we identified a significant increase in α-band FC post-stimulation (T1>T0). The ML analysis identified an optimal differential network at a threshold of $t = 2.8$ ($p = 0.043$, accuracy = 0.75 [0.73–0.76]) (Fig. 5, panels A, B, C). This network included 23 nodes and 26 links and was well distributed between the two hemispheres (52.2 % right). ROIs with the highest degree were located in prefrontal cortex (bilateral superior frontal regions, right caudal and rostral middle frontal gyri), insula (left), sensorimotor areas (bilateral precentral and paracentral areas), temporal, limbic (notably right entorhinal), and occipital regions (left lingual and right lateral occipital). The most represented connections involved fronto-sensorimotor (15.4 %), intra-frontal (13.5 %), and occipito-frontal (9.6 %) links. The mNC was significantly higher in T1 compared to T0 (T0 0.12 ± 0.04, T1 0.24 ± 0.11, $p < 0.001$), indicating increased network connectivity after stimulation (Fig. 5, panel D).

We also identified a significant decrease in β-band FC post-stimulation. The ML analysis identified the optimal differential network at $t = 2.1$ ($p = 0.048$, accuracy = 0.74 [0.73–0.76]) (Fig. 5, panels F, G, H). This network comprised 52 nodes and 83 links and was bilaterally distributed, with a modest right-hemispheric prevalence (57.7 %). ROIs with the highest degree were part of sensorimotor (bilateral paracentral and right pre and postcentral gyri), temporal (right superior temporal sulcus and entorhinal cortex), parietal (right superior and inferior parietal gyri, right precuneus), limbic (left isthmus cingulate and right parahippocampus) and prefrontal (bilateral superior frontal regions and ventrolateral prefrontal cortex). The most represented connections were fronto-temporal (16.9 %), temporo-limbic (13.3 %), and intra-frontal (10.8 %). Accordingly, the mNC was significantly lower in T1 compared to T0 (T0 0.14 ± 0.07, T1 0.07 ± 0.03, $p < 0.001$) (Fig. 5, panel I).

No other significant FC changes were observed across the remaining frequency bands in the OFF state. Similarly, sham tDCS produced no FC differences.

3.6. Graph-theoretical analysis of functional changes after tDCS in PD

Since we identified significant differences in FC at both α and β bands between T0 and T1 using NBS, we further investigated the intrinsic topological properties of the whole-brain functional organization through graph-theoretical analysis. In the α-band, we observed a significant increase in global efficiency following anodal tDCS (T0: 0.14 ± 0.05; T1: 0.17 ± 0.07; $p = 0.046$), while a significant decrease was found in scale-freeness (T0 0.69 ± 0.27, T1 0.52 ± 0.29; $p = 0.032$). No significant differences were found in transitivity (T0 0.11 ± 0.06, T1 0.12 ± 0.06, $p = 0.16$) and assortativity (T0 -0.10 ± 0.10, T1 -0.12 ± 0.09, $p = 0.53$) (Fig. 5, panel E).

In the β-band, we found a significant decrease in scale-freeness (T0 0.79 ± 0.22; T1 0.65 ± 0.20; $p = 0.029$), whereas no other global graph metrics showed significant differences (global efficiency T0 0.11 ± 0.06, T1 0.09 ± 0.04; $p = 0.20$; transitivity T0 0.07 ± 0.03, T1 0.06 ± 0.02, $p = 0.16$; assortativity T0 -0.04 ± 0.08, T1 – 0.07 ± 0.08, $p = 0.11$) (Fig. 5, panel J).

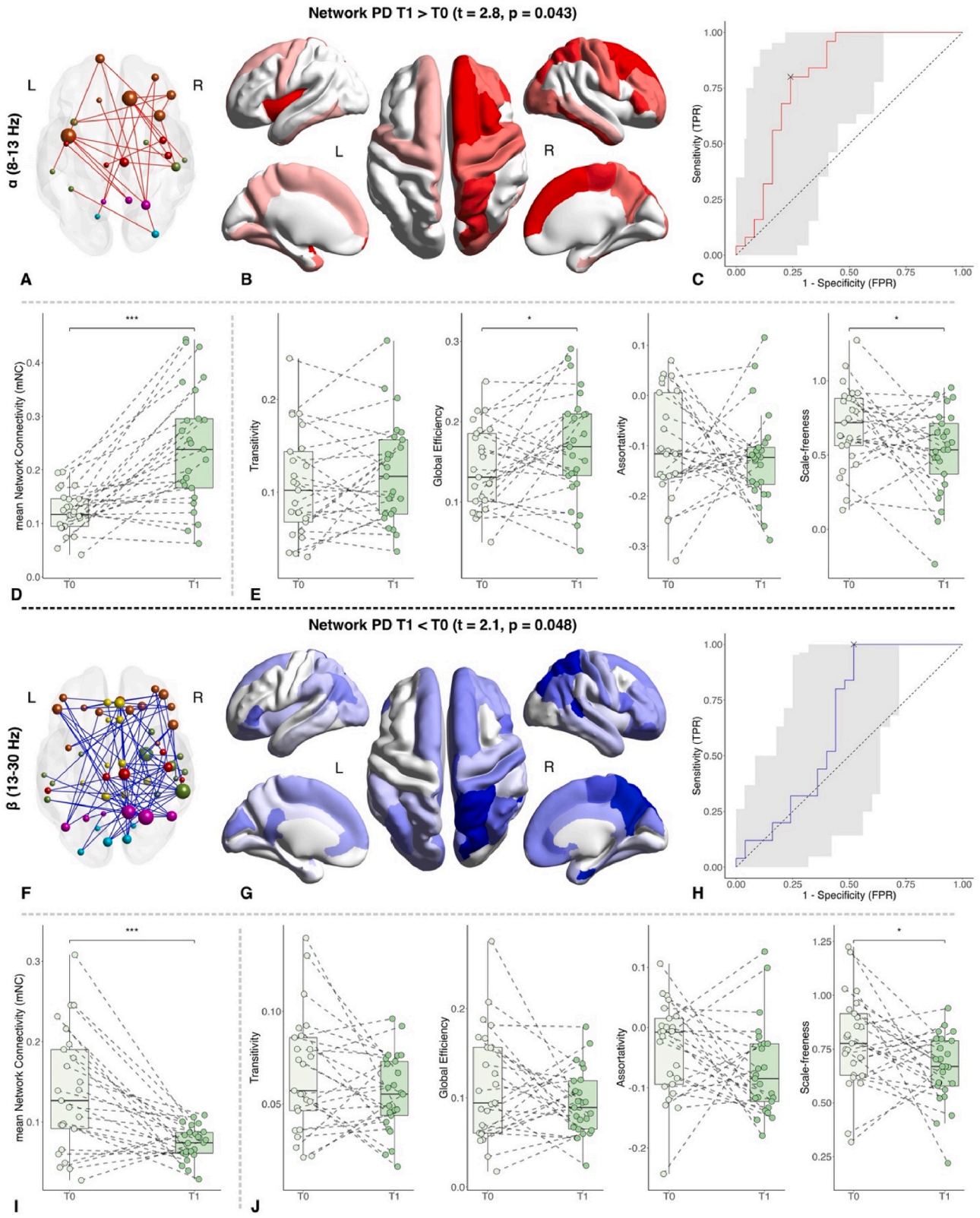

Fig. 5. Graph representation of the differential network in α band (**A**) and in β band (**F**) between T0 and T1 in PD patients treated with Anodal tDCS. The color of spheres represents different brain lobes: orange = fronto-insular, red = sensorimotor, yellow = limbic, green = temporal, magenta = parietal, light-blue = occipital; sphere diameters are directly proportional to region of interest (ROI) degrees. Map representation of ROI degrees on model brain surface of the differential network in α band (**B**) and in β band (**G**). ROC curve indicating the predictive performance (T0 vs T1) of the identified NBS network in α (**C**) and in β (**H**). Box plots represent the mNC values in T0 vs T1 of the differential network in α band (**D**) and in β band (**I**). Box plots of global graph metrics (Transitivity, Global Efficiency, Assortativity, Scale-Freeness) comparing T0 and T1 α band network (**E**) and in β band network (**J**).

3.7. Correlations between functional changes and clinical outcomes

We examined correlations between the increase of α-band network mNC and changes in clinical scores following stimulation in the PD group. Greater increases in α-band mNC were significantly associated with improved cognitive performance ($r = 0.43$, $p = 0.031$, BS-95 %CI [0.00 0.75]), reductions in non-motor symptoms (NMSS: $r = -0.41$, $p = 0.0041$, BS-95 %CI [−0.67 -0.04]), and improvement in gait symptoms ($r = -0.39$, $p = 0.048$, BS-95 %CI [−0.67 -0.03]). Moreover, decreases in β-band mNC were significantly associated with improved bradykinesia ($r = 0.42$, $p = 0.034$ BS-95 %CI [−0.06 0.76]) (Fig. 6).

4. Discussion

This study aimed to investigate the biological and network-level effects of an anodal M1 tDCS protocol in patients with intermediate-stage PD, by analyzing both clinical outcomes and changes in EEG-based FC. Notably, the stimulation protocol induced significant clinical improvement in the OFF-state, which was accompanied by consistent changes in FC, affecting both extrinsic network configuration and intrinsic topological properties, as revealed by combined NBS and graph-theoretical analysis. These findings provide novel insights into the mechanisms by which anodal tDCS may exert its neuromodulatory effects in PD, supporting its integration as a therapeutic tool in clinical practice.

As a necessary preliminary step of the study, we first outlined the baseline FC profile of the PD population in comparison to HC. PD patients exhibited reduced α-band FC within a network involving prefrontal, sensorimotor, and temporal regions, which was significantly associated with worse gait performance, higher burden of non-motor symptoms, and poorer cognitive function. PD patients also showed increased β-band FC in a network primarily involving sensorimotor, limbic, and parietal regions, which was correlated with more severe bradykinesia. Overall, such baseline features were consistent with the existing literature suggesting the cholinergic signaling impairment and the dopaminergic depletion behind the abnormalities in the α-band [32,55–59] and β-band respectively [32,57,59–61].

In addition, we applied a graph-theoretical analysis to identify changes even in the whole-brain network organization in PD patients at baseline. Compared to controls, PD patients had reduced transitivity and global efficiency in the α-band, probably reflecting impaired functional segregation and integration, as reported in previous studies [62–64]. Conversely, the α-band assortativity was significantly increased, suggesting a potential compensatory reorganization toward a more resilient structure. No significant group differences were found in scale-freeness, revealing an overall preservation of the hub-based architecture of the network. Regarding the β-band, PD patients showed increased transitivity and global efficiency, which may indicate a network reorganization with stronger local clustering and more efficient short-range communication, consistent with either compensatory adaptations or the pathological β-band hypersynchronization.

After observing that the motor and non-motor disturbances in our PD population originate from, or at least reflect, band-specific dysfunctional networks, we investigated the clinical and neurophysiological effects of anodal M1 tDCS. We found that the stimulation protocol induced a relevant amelioration in non-motor symptoms and cognitive performance, which is in line with other previous works [14–18]. The stimulation also improved the overall OFF-state motor syndrome, as well as the bradykinesia, tremor, and gait/postural subdomains, specifically, while leaving the ON-state motor burden unaffected. Rigidity subdomain was not modified, probably because it may be driven by subcortical circuits [65] and altered muscle viscoelastic properties, which are features less directly influenced by cortical neuromodulation. The peculiar OFF-state improvement suggests that, at an intermediate disease stage, anodal M1 tDCS may exert consistent yet subtle effects on PD motor function, as far as detectable by the MDS-UPDRS. Indeed, at this stage, dopaminergic replacement through oral medications can still ensure the so-called “best ON” [66], which may mask any additional, clinically detectable, beneficial effects in the ON state deriving from neuromodulation.

Indeed, when examining the changes in EEG-based FC following stimulation, we observed in the OFF-state a significant increase in α-band FC within a network encompassing sensorimotor, prefrontal, and insular cortices, alongside a decrease in β-band FC within a network primarily involving sensorimotor, limbic, and temporo-parietal regions. Notably, the enhancement of α-band FC correlated with improvement in gait/postural scores, NMSS and PD-CRS, whereas the reduction in the β-band hypersynchronization correlated with slight amelioration of bradykinesia. Anodal stimulation over M1 is known to enhance cortical excitability, potentially activating descending corticospinal and cortico-brainstem pathways [28,29], influencing the motor output and indirectly modulating subcortico-cortical circuits involved in PD symptoms pathophysiology. In addition, our data suggest that low-intensity direct current stimulation may facilitate thalamo-cortical interplay and cholinergic transmission [56,67] and reduce the excessive subcortico-cortical coupling arising from the dopaminergic deficiency [68]. Therefore, anodal M1 tDCS may induce clinical benefits at intermediate PD stages by rebalancing disrupted oscillatory patterns and restoring dysfunctional pathways that lead to main motor and non-motor symptoms.

Finally, we analyzed the effects of tDCS on network topography. This analysis revealed a reduction in the scale-free organization in both the α and β-band functional connectomes. This change was accompanied by increased global efficiency in the α-band network. Previous studies investigating the effects of tDCS on brain networks using graph theoretical measures have reported heterogeneous outcomes, including an increase in clustering coefficient, indicative of enhanced network

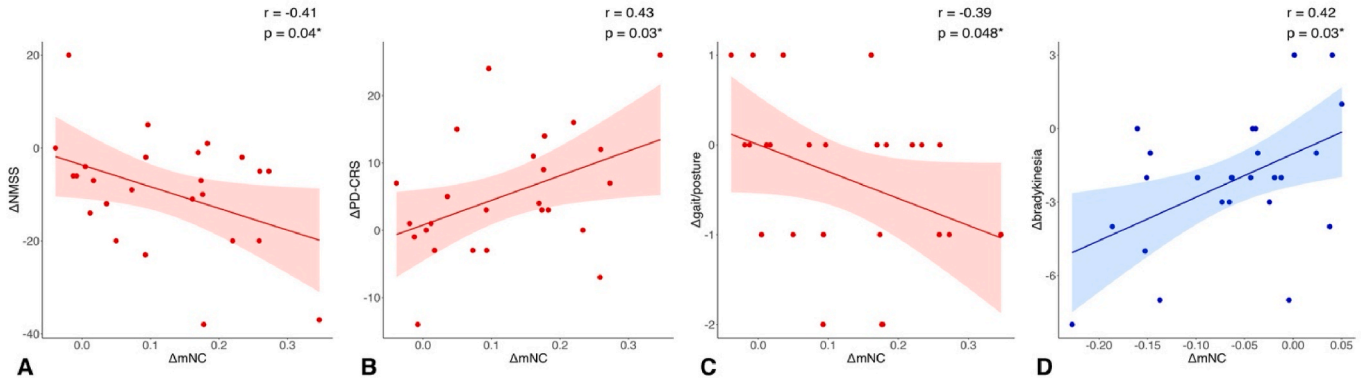

Fig. 6. Scatter plots illustrating correlations between differential ΔmNC of α-band network (T1-T0) and ΔNMSS (**A**), ΔPD-CRS (**B**), and Δgait/posture subscore (**C**), and ΔmNC of β-band network and Δbradykinesia (**D**).

segregation [69], an increase in minimum path length, suggesting reduced long-range connectivity coupled with strengthened short-range interactions [70], or no significant changes [71]. Moreover, recent evidence derived from mathematical modeling suggests that tDCS intensity differentially impacts brain network organization, with higher intensities potentially diminishing small-world characteristics [72]. Our results suggest that tDCS may help restore FC toward a more physiological range by enhancing α-band and reducing β-band connectivity, although in a diffuse and non-selective manner, which broadly improves connectivity across the network rather than targeting specific functional hubs. Therefore, the stimulation may enhance communication among regions within the network, but at the cost of disrupting its intrinsic hierarchical organization. In turn, such a widespread, undifferentiated increase in node activity could account for the post-tDCS reduction in scale-freeness, reflecting either a loss of hub dominance within the network architecture or a redistribution toward a more random topology. While the precise clinical significance of this phenomenon remains to be determined, both interpretations suggest that non-selective stimulation may reduce network robustness, which supports the idea that more targeted approaches, particularly those focusing on hub regions, could preserve scale-free properties and potentially enhance therapeutic efficacy.

This study has some limitations. The relatively small sample size, the specific inclusion of intermediate-stage PD, and the absence of longitudinal follow-up may limit the generalizability of the findings. However, all patients were carefully selected to represent a clinically homogeneous group, minimizing variability related to disease progression and treatment response. Regarding motor outcomes, we found a modest but significant improvement in the OFF state, whereas no effect was observed in the ON state. These findings highlight that future tDCS trials should consider outcome measures capable of capturing more subtle yet clinically meaningful changes in motor function or quality of life, since standard clinical scales may only partially reflect treatment effects. Nevertheless, the OFF-state improvement in MDS-UPDRS III, although small, was significant, supported by the randomized sham-controlled design, and correlated with the changes in FC. Taken together, this finding provides valuable mechanistic insights into the potential of tDCS in PD. Finally, although HD-EEG and graph-theoretical approaches are powerful tools for investigating large-scale brain network dynamics, source localization and FC estimates remain indirect and rely on specific modeling assumptions. Despite these limitations, the rigorous design and the integrated clinical–neurophysiological approach strengthen the validity of our findings, helping to address the heterogeneity observed in previous studies on tDCS in PD.

5. Conclusions

This study provides new evidence that anodal M1-tDCS in PD modulates large-scale brain network FC, closely linked to clinical improvement. tDCS appears to exert its effects by enhancing α-band FC in prefrontal and sensorimotor circuits, possibly reflecting an improvement in cholinergic pathways, and by reducing pathological β-band cortical hypersynchronization, a hallmark of dopaminergic dysfunction in PD. tDCS also seems to alter the topological organization of brain networks, suggesting a broader effect on network architecture.

By integrating HD-EEG, NBS and graph theory analysis, our findings suggest that tDCS may promote functional reorganization of disease-relevant circuits, supporting network-level biomarkers as tools to guide future adaptive, frequency-targeted neuromodulation. Closed-loop strategies based on neurophysiological signatures may further optimize interventions across PD symptoms. These insights reinforce tDCS as a promising complementary option in intermediate-stage PD, when drug efficacy declines but advanced therapies are not yet indicated.

CRediT authorship contribution statement

Clara Simonetta: Writing – original draft, Visualization, Methodology, Investigation, Formal analysis, Data curation, Conceptualization. **Matteo Conti:** Writing – review & editing, Writing – original draft, Visualization, Software, Methodology, Investigation, Formal analysis, Conceptualization. **Jacopo Bissacco:** Resources, Investigation, Data curation. **Valerio Ferrari:** Investigation, Data curation. **Chiara Salimei:** Investigation, Data curation. **Federico Carparelli:** Investigation, Data curation. **Silvio Bagetta:** Investigation, Data curation. **Davide Mascioli:** Investigation, Data curation. **Veronica Buttarazzi:** Investigation, Data curation. **Maria Mancini:** Investigation, Data curation. **Francesca Di Giuliano:** Writing – review & editing, Supervision. **Nicola Biagio Mercuri:** Supervision, Project administration, Funding acquisition. **Mariangela Pierantozzi:** Supervision, Funding acquisition. **Alessandro Stefani:** Writing – review & editing, Supervision, Project administration, Funding acquisition. **Tommaso Schirinzi:** Writing – review & editing, Supervision, Project administration, Funding acquisition, Conceptualization.

Funding

This study was supported by Fondazione Baroni grant and Banca D'Italia grant to TS. The research has also received funding from the European Union (NextGenerationEU) through the Italian Ministry of University and Research (MUR) under PNRR–M4C2-I1.3 Project PE_00000019 "Heal Italia" to T.S. and M.P. The work was also supported by #NEXTGENERATIONEU (NGEU) and funded by the Ministry of University and Research (MUR), National Recovery and Resilience Plan (NRRP), project MNESYS (PE0000006) – A Multiscale integrated approach to the study of the nervous system in health and disease (DN. 1553 October 11, 2022) to NBM, and BRIC 2023 (INAIL) to AS. The views and opinions expressed are those of the authors only and do not necessarily reflect those of the European Union or the European Commission.

Declaration of competing interest

The authors declare that they have no known competing financial interests or personal relationships that could have appeared to influence the work reported in this paper.

Acknowledgments

None.

Appendix A. Supplementary data

Supplementary data to this article can be found online at https://doi.org/10.1016/j.brs.2025.10.016.

Data availability

The raw data supporting the conclusions of this article will be made available by the authors upon reasonable request.

References

[1] Bloem BR, Okun MS, Klein C, Bloem BR, Okun MS, Klein C. Parkinson's disease. Lancet 2021;397(10291):2284–303. Vol. 397, The Lancet. 2021.
[2] Herrington TM, Briscoe J, Eskandar E. Structural and functional network dysfunction in Parkinson disease. Radiology 2017;285.
[3] Rajan R, Garg K, Srivastava AK, Singh M. Device-assisted and neuromodulatory therapies for Parkinson's disease: a network meta-analysis. Mov Disord 2022;37.
[4] Schröter N, Sajonz BEA, Jost WH, Rijntjes M, Coenen VA, Groppa S. Advanced therapies in Parkinson's disease: an individualized approach to their indication. J Neural Transm 2024 Nov 13;131(11):1285–93.

[5] Chan MMY, Yau SSY, Han YMY. The neurobiology of prefrontal transcranial direct current stimulation (tDCS) in promoting brain plasticity: a systematic review and meta-analyses of human and rodent studies. Neurosci Biobehav Rev 2021;125.
[6] Guerra A, Asci F, D'Onofrio V, Sveva V, Bologna M, Fabbrini G, et al. Enhancing gamma oscillations restores primary motor cortex plasticity in Parkinson's disease. J Neurosci 2020;40(24):4788–96.
[7] Fregni F, Boggio PS, Santos MC, Lima M, Vieira AL, Rigonatti SP, et al. Noninvasive cortical stimulation with transcranial direct current stimulation in Parkinson's disease. Mov Disord 2006;21(10).
[8] Salimpour Y, Mari ZK, Shadmehr R. Altering effort costs in Parkinson's disease with noninvasive cortical stimulation. J Neurosci 2015;35(35).
[9] Schoellmann A, Scholten M, Wasserka B, Govindan RB, Krüger R, Gharabaghi A, et al. Anodal tDCS modulates cortical activity and synchronization in Parkinson's disease depending on motor processing. Neuroimage Clin 2019;22.
[10] Valentino F, Cosentino G, Brighina F, Pozzi NG, Sandrini G, Fierro B, et al. Transcranial direct current stimulation for treatment of freezing of gait: a cross-over study. Mov Disord 2014;29(8).
[11] Zhang B, Huang F, Liu J, Zhang D. Bilateral transcranial direct current stimulation may be a feasible treatment of Parkinsonian tremor. Front Neurosci 2023;17.
[12] Beretta VS, Orcioli-Silva D, Conceição NR, Nóbrega-Sousa P, Pereira MP, Gobbi LTB, et al. tDCS application for postural control in Parkinson's disease: effects are associated with baseline characteristics. Parkinsonism Relat Disord 2021;93.
[13] Dagan M, Herman T, Harrison R, Zhou J, Giladi N, Ruffini G, et al. Multitarget transcranial direct current stimulation for freezing of gait in Parkinson's disease. Mov Disord 2018;33(4).
[14] Aksu S, Uslu A, İşçen P, Tülay EE, Barham H, Soyata AZ, et al. Does transcranial direct current stimulation enhance cognitive performance in Parkinson's disease mild cognitive impairment? An event-related potentials and neuropsychological assessment study. Neurol Sci 2022;43(6).
[15] Firouzi M, Van Herk K, Kerckhofs E, Swinnen E, Baeken C, Van Overwalle F, et al. Transcranial direct-current stimulation enhances implicit motor sequence learning in persons with Parkinson's disease with mild cognitive impairment. J Neuropsychol 2021;15(3).
[16] Pereira JB, Junqué C, Bartrés-Faz D, Martí MJ, Sala-Llonch R, Compta Y, et al. Modulation of verbal fluency networks by transcranial direct current stimulation (tDCS) in Parkinson's disease. Brain Stimul 2013;6(1).
[17] Simonetta C, Bissacco J, Conti M, Bovenzi R, Salimei C, Cerroni R, et al. Motor cortex transcranial direct current stimulation improves non-motor symptoms in early-onset Parkinson's disease: a pilot study. J Neural Transm 2024;131(2).
[18] Benussi A, Alberici A, Cantoni V, Manenti R, Brambilla M, Dell'Era V, et al. Modulating risky decision-making in Parkinson's disease by transcranial direct current stimulation. Eur J Neurol 2017;24(5).
[19] Benninger DH, Lomarev M, Lopez G, Wassermann EM, Li X, Considine E, et al. Transcranial direct current stimulation for the treatment of Parkinson's disease. J Neurol Neurosurg Psychiatry 2010;81(10).
[20] Sadler CM, Kami AT, Nantel J, Lommen J, Carlsen AN. Transcranial direct current stimulation over motor areas improves reaction time in Parkinson's disease. Front Neurol 2022;13.
[21] Swank C, Mehta J, Criminger C. Transcranial direct current stimulation lessens dual task cost in people with Parkinson's disease. Neurosci Lett 2016;626.
[22] Doruk D, Gray Z, Bravo GL, Pascual-Leone A, Fregni F. Effects of tDCS on executive function in Parkinson's disease. Neurosci Lett 2014;582.
[23] Elder GJ, Ashcroft J, da Silva Morgan K, Umme Kulsum M, Banerjee R, Chatterjee P, et al. Transcranial direct current stimulation in Parkinson's disease dementia: a randomised double-blind crossover trial. Brain Stimul 2017;10.
[24] Elsner B, Kugler J, Pohl M, Mehrholz J. Transcranial direct current stimulation (tDCS) for idiopathic Parkinson's disease. Cochrane Database Syst Rev 2016;2016.
[25] Goodwill AM, Lum JAG, Hendy AM, Muthalib M, Johnson L, Albein-Urios N, et al. Using non-invasive transcranial stimulation to improve motor and cognitive function in Parkinson's disease: a systematic review and meta-analysis. Sci Rep 2017;7.
[26] Liu X, Liu H, Liu Z, Rao J, Wang J, Wang P, et al. Transcranial direct current stimulation for Parkinson's disease: a systematic review and meta-analysis. Front Aging Neurosci 2021;13.
[27] Zhang X, Jing F, Liu Y, Tang J, Hua X, Zhu J, et al. Effects of non-invasive brain stimulation on walking and balance ability in Parkinson's patients: a systematic review and meta-analysis. Front Aging Neurosci 2023 Jan 10;14.
[28] Nitsche MA, Paulus W. Excitability changes induced in the human motor cortex by weak transcranial direct current stimulation. J Physiol (Paris) 2000;527(3).
[29] Priori A, Berardelli A, Rona S, Accornero N, Manfredi M. Polarization of the human motor cortex through the scalp. Neuroreport 1998;9(10).
[30] Kuo HI, Bikson M, Datta A, Minhas P, Paulus W, Kuo MF, et al. Comparing cortical plasticity induced by conventional and high-definition 4 × 1 ring tDCS: a neurophysiological study. Brain Stimul 2013;6(4).
[31] Conti M, Bovenzi R, Garasto E, Schirinzi T, Placidi F, Mercuri NB, et al. Brain Functional Connectivity in de novo Parkinson's Disease Patients Based on Clinical EEG. Front Neurol 2022;13.
[32] Conti M, D'Onofrio V, Bovenzi R, Ferrari V, Di Giuliano F, Cerroni R, et al. Cortical functional connectivity changes in the body-first and brain-first subtypes of Parkinson's disease. Mov Disord 2025 Feb;40(2):254–65.
[33] Utianski RL, Caviness JN, van Straaten ECW, Beach TG, Dugger BN, Shill HA, et al. Graph theory network function in parkinson's disease assessed with electroencephalography. Clin Neurophysiol 2016;127(5).
[34] Kim J, Criaud M, Cho SS, Díez-Cirarda M, Mihaescu A, Coakeley S, et al. Abnormal intrinsic brain functional network dynamics in Parkinson's disease. Brain 2017;140 (11).
[35] Miraglia F, Vecchio F, Pappalettera C, Nucci L, Cotelli M, Judica E, et al. Brain connectivity and graph theory analysis in Alzheimer's and Parkinson's disease: the contribution of electrophysiological techniques. Brain Sci 2022;12.
[36] Barabási AL. Scale-free networks: a decade and beyond. Science 2009;325.
[37] Mijalkov M, Volpe G, Pereira JB. Directed brain connectivity identifies widespread functional network abnormalities in Parkinson's disease. Cerebr Cortex 2022;32 (3).
[38] Cerasa A, Novellino F, Quattrone A. Connectivity changes in Parkinson's disease. Curr Neurol Neurosci Rep 2016;16.
[39] Postuma RB, Berg D, Stern M, Poewe W, Olanow CW, Oertel W, et al. MDS clinical diagnostic criteria for Parkinson's disease. Mov Disord 2015;30.
[40] Poewe W, Gauthier S, Aarsland D, Leverenz JB, Barone P, Weintraub D, et al. Diagnosis and management of Parkinson's disease dementia. Int J Clin Pract 2008; 62.
[41] Aslam S, Manfredsson F, Stokes A, Shill H. "Advanced" Parkinson's disease: a review. Parkinsonism and related disorders, vol 123; 2024.
[42] Antonini A, Stoessl AJ, Kleinman LS, Skalicky AM, Marshall TS, Sail KR, et al. Developing consensus among movement disorder specialists on clinical indicators for identification and management of advanced Parkinson's disease: a multi-country Delphi-panel approach. Curr Med Res Opin 2018;34(12).
[43] Woods AJ, Antal A, Bikson M, Boggio PS, Brunoni AR, Celnik P, et al. A technical guide to tDCS, and related non-invasive brain stimulation tools, vol 127. Clinical Neurophysiology; 2016.
[44] Antal A, Alekseichuk I, Bikson M, Brockmöller J, Brunoni AR, Chen R, et al. Low intensity transcranial electric stimulation: safety, ethical, legal regulatory and application guidelines. Clin Neurophysiol 2017;128.
[45] Nitsche MA, Lampe C, Antal A, Liebetanz D, Lang N, Tergau F, et al. Dopaminergic modulation of long-lasting direct current-induced cortical excitability changes in the human motor cortex. Eur J Neurosci 2006;23(6).
[46] Jost ST, Kaldenbach MA, Antonini A, Martinez-Martin P, Timmermann L, Odin P, et al. Levodopa dose equivalency in Parkinson's disease: updated systematic review and proposals. Mov Disord 2023;38(7).
[47] Berganzo K, Tijero B, González-Eizaguirre A, Somme J, Lezcano E, Gabilondo I, et al. Motor and non-motor symptoms of Parkinson's disease and their impact on quality of life and on different clinical subgroups [Internet]. Available from, www.elsevier.es/neurologia; 2016.
[48] Chaudhuri KR, Martinez-Martin P, Brown RG, Sethi K, Stocchi F, Odin P, et al. The metric properties of a novel non-motor symptoms scale for Parkinson's disease: results from an international pilot study. Mov Disord 2007;22(13).
[49] Kulisevsky J, Fernández de Bobadilla R, Pagonabarraga J, Martínez-Horta S, Campolongo A, García-Sánchez C, et al. Measuring functional impact of cognitive impairment: validation of the Parkinson's disease cognitive functional rating scale. Parkinsonism Relat Disord 2013;19(9).
[50] Yassine S, Gschwandtner U, Auffret M, Achard S, Verin M, Fuhr P, et al. Functional brain dysconnectivity in Parkinson's disease: a 5-Year longitudinal study. Mov Disord 2022;37(7):1444–53.
[51] Hyvärinen A, Oja E. Independent component analysis: algorithms and applications. Neural Netw 2000;13(4–5).
[52] Hardmeier M, Hatz F, Bousleiman H, Schindler C, Stam CJ, Fuhr P. Reproducibility of functional connectivity and graph measures based on the phase lag index (PLI) and weighted phase lag index (wPLI) derived from high resolution EEG. PLoS One 2014;9(10).
[53] Zalesky A, Fornito A, Bullmore ET. Network-based statistic: identifying differences in brain networks. Neuroimage 2010;53(4).
[54] Faul F, Erdfelder E, Lang AG, Buchner A. G*Power 3: a flexible statistical power analysis program for the social, behavioral, and biomedical sciences. In: Behavior research methods; 2007.
[55] Pugnetti L, Baglio F, Farina E, Alberoni M, Calabrese E, Gambini A, et al. EEG evidence of posterior cortical disconnection in PD and related dementias. Int J Neurosci 2010;120(2).
[56] Babiloni C, Del Percio C, Lizio R, Noce G, Lopez S, Soricelli A, et al. Functional cortical source connectivity of resting state electroencephalographic alpha rhythms shows similar abnormalities in patients with mild cognitive impairment due to Alzheimer's and Parkinson's diseases. Clin Neurophysiol 2018;129(4).
[57] Hassan M, Chaton L, Benquet P, Delval A, Leroy C, Plomhause L, et al. Functional connectivity disruptions correlate with cognitive phenotypes in Parkinson's disease. Neuroimage Clin 2017;14.
[58] Klassen BT, Hentz JG, Shill HA, Driver-Dunckley E, Evidente VGH, Sabbagh MN, et al. Quantitative EEG as a predictive biomarker for Parkinson disease dementia. Neurology 2011;77(2).
[59] Ponsen MM, Stam CJ, Bosboom JLW, Berendse HW, Hillebrand A. A three dimensional anatomical view of oscillatory resting-state activity and functional connectivity in Parkinson's disease related dementia: an MEG study using atlas-based beamforming. Neuroimage Clin 2013;2(1).
[60] Tinkhauser G, Torrecillos F, Duclos Y, Tan H, Pogosyan A, Fischer P, et al. Beta burst coupling across the motor circuit in Parkinson's disease. Neurobiol Dis 2018; 117.
[61] Bosch TJ, Espinoza AI, Mancini M, Horak FB, Singh A. Functional connectivity in patients With Parkinson's disease and freezing of gait using resting-state EEG and graph theory. Neurorehabil Neural Repair 2022;36(10–11).
[62] Olde Dubbelink KTE, Hillebrand A, Stoffers D, Deijen JB, Twisk JWR, Stam CJ, et al. Disrupted brain network topology in Parkinson's disease: a longitudinal magnetoencephalography study. Brain 2014;137(1).

[63] Li Z, Liu C, Wang Q, Liang K, Han C, Qiao H, et al. Abnormal functional brain network in Parkinson's disease and the effect of acute deep brain stimulation. Front Neurol 2021;12.
[64] Zuo C, Suo X, Lan H, Pan N, Wang S, Kemp GJ, et al. Global alterations of whole brain structural connectome in Parkinson's disease: a meta-analysis. Neuropsychol Rev 2023;33.
[65] Asci F, Falletti M, Zampogna A, Patera M, Hallett M, Rothwell J, et al. Rigidity in Parkinson's disease: evidence from biomechanical and neurophysiological measures. Brain 2023;146(9).
[66] Alonso-Canovas A, Voeten J, Gifford L, Thomas O, Lees AJ, Bloem BR. The early treatment phase in Parkinson's disease: not a honeymoon for all, not a honeymoon at all?, vol. 13. Journal of Parkinson's Disease; 2023.
[67] Schumacher J, Thomas AJ, Peraza LR, Firbank M, Cromarty R, Hamilton CA, et al. EEG alpha reactivity and cholinergic system integrity in Lewy body dementia and Alzheimer's disease. Alzheimers Res Ther 2020;12(1).
[68] Conti M, Guerra A, Pierantozzi M, Bovenzi R, D'Onofrio V, Simonetta C, et al. Band-specific altered cortical connectivity in early Parkinson's disease and its clinical correlates. Mov Disord 2023 Dec 20;38(12):2197–208.
[69] Cao J, Liu H. Modulating the resting-state functional connectivity patterns of language processing areas in the human brain with anodal transcranial direct current stimulation applied over the Broca's area. Neurophotonics 2018;5(2).
[70] Polanía R, Paulus W, Antal A, Nitsche MA. Introducing graph theory to track for neuroplastic alterations in the resting human brain: a transcranial direct current stimulation study. Neuroimage 2011;54(3).
[71] Mancini M, Brignani D, Conforto S, Mauri P, Miniussi C, Pellicciari MC. Assessing cortical synchronization during transcranial direct current stimulation: a graph-theoretical analysis. Neuroimage 2016;140.
[72] Shao H, Gu G, Guo X, Li X, Cui D. Nonlinear dose-response relationship in tDCS-induced brain network synchrony: a resting-state whole-brain model analysis. Comput Methods Progr Biomed 2025 May 1:263.